University of Mississippi

eGrove

Faculty and Student Publications | Pharmacy, School of

1-1-2021

Exploring the chemical space of 1,2,3-triazolyl triclosan analogs for discovery of new antileishmanial chemotherapeutic agents

Julia Fernández de Luco
Consejo Nacional de Investigaciones Científicas y Técnicas

Alejandro I. Recio-Balsells
Consejo Nacional de Investigaciones Científicas y Técnicas

Diego G. Ghiano
Consejo Nacional de Investigaciones Científicas y Técnicas

Ana Bortolotti
Universidad Nacional de Rosario, Facultad de Ciencias Medicas

Follow this and additional works at: https://egrove.olemiss.edu/pharmacy_facpubs

 Part of the Pharmacy and Pharmaceutical Sciences Commons

Recommended Citation

Fernández De Luco, J., Recio-Balsells, A. I., Ghiano, D. G., Bortolotti, A., Belardinelli, J. M., Liu, N., Hoffmann, P., Lherbet, C., Tonge, P. J., Tekwani, B., Morbidoni, H. R., & Labadie, G. R. (2021). Exploring the chemical space of 1,2,3-triazolyl triclosan analogs for discovery of new antileishmanial chemotherapeutic agents. RSC Medicinal Chemistry, 12(1), 120–128. https://doi.org/10.1039/D0MD00291G

This Article is brought to you for free and open access by the Pharmacy, School of at eGrove. It has been accepted for inclusion in Faculty and Student Publications by an authorized administrator of eGrove. For more information, please contact egrove@olemiss.edu.

RSC Medicinal Chemistry

ROYAL SOCIETY OF CHEMISTRY

RESEARCH ARTICLE

View Article Online
View Journal | View Issue

Check for updates

Cite this: *RSC Med. Chem.*, 2021, **12**, 120

Exploring the chemical space of 1,2,3-triazolyl triclosan analogs for discovery of new antileishmanial chemotherapeutic agents†

Julia Fernández de Luco, ‡[a] Alejandro I. Recio-Balsells, ‡[a] Diego G. Ghiano,‡[a] Ana Bortolotti,[b] Juán Manuel Belardinelli,§[b] Nina Liu,[c] Pascal Hoffmann,[d] Christian Lherbet,[d] Peter J. Tonge, [c] Babu Tekwani,¶[e] Héctor R. Morbidoni *[bf] and Guillermo R. Labadie *[ag]

Received 13th August 2020,
Accepted 13th October 2020

DOI: 10.1039/d0md00291g

rsc.li/medchem

Published on 05 November 2020. Downloaded on 9/20/2023 4:42:31 PM.

Triclosan and isoniazid are known antitubercular compounds that have proven to be also active against *Leishmania* parasites. On these grounds, a collection of 37 diverse 1,2,3-triazoles based on the antitubercular molecules triclosan and 5-octyl-2-phenoxyphenol (8PP) were designed in search of novel structures with leishmanicidal activity and prepared using different alkynes and azides. The 37 compounds were assayed against *Leishmania donovani*, the etiological agent of leishmaniasis, yielding some analogs with activity at micromolar concentrations and against *M. tuberculosis* H37Rv resulting in scarce active compounds with an MIC of 20 μM. To study the mechanism of action of these catechols, we analyzed the inhibition activity of the library on the *M. tuberculosis* enoyl-ACP reductase (ENR) InhA, obtaining poor inhibition of the enzyme. The cytotoxicity against Vero cells was also tested, resulting in none of the compounds being cytotoxic at concentrations of up to 20 μM. Derivative **5f** could be considered a valuable starting point for future antileishmanial drug development. The validation of a putative leishmanial InhA orthologue as a therapeutic target needs to be further investigated.

1. Introduction

Neglected tropical diseases (NTDs) are an ever-growing list of treatable and preventable diseases that proliferate in impoverished environments. One of the most relevant characteristics of NTDs is their global impact being present in every continent. NTDs are usually emergent in regions lacking adequate hygienic conditions and many of them are vector-borne. Tropical and subtropical areas where the climate conditions are hot and humid are the most affected, due to the combination of the presence of many vectors and poor living conditions.

Leishmaniasis is one of the most concerning vector-borne NTDs, an expanding endemic disease caused by the protozoan parasite *Leishmania* spp. and transmitted by over 90 phlebotomine sand fly species. Visceral leishmaniasis (VL), or kala-azar, is the most severe form of the disease which, if not treated, has a mortality rate close to 100%, surpassing 30 000 deaths per year. Unfortunately, there is no vaccine available and the regular treatment includes drugs that are toxic to the host, so they are used at low doses ending in the generation of drug resistant forms of the parasite.

The World Health Organization (WHO) has reported a rate of 1.3 million cases of leishmaniasis per year and 350 million people exposed to infections.[1] This fact has alerted the scientific community and driven it to the urgent search for new effective and less toxic drugs with novel structures and different targets.

Bacterial fatty acid biosynthesis is a validated target for drug discovery;[2] however, it has not been fully exploited. An

[a] *Instituto de Química Rosario, UNR, CONICET, Suipacha 531, S2002LRK, Rosario, Argentina. E-mail: labadie@iquir-conicet.gov.ar; Fax: +54 341 4370477; Tel: +54 341 4370477*
[b] *Laboratorio de Microbiología Molecular, Facultad de Ciencias Médicas, Universidad Nacional de Rosario, Santa Fe 3100, S2002KTR, Rosario, Argentina. E-mail: morbiatny@yahoo.com*
[c] *Department of Chemistry, Institute of Chemical Biology & Drug Discovery, Stony Brook University, Stony Brook, NY 11794, USA*
[d] *LSPCMIB, UMR-CNRS 5068, Université Paul Sabatier-Toulouse III, 118 Route de Narbonne, 31062 Toulouse Cedex 9, France*
[e] *National Center for Natural Products Research & Department of Biomolecular Sciences, School of Pharmacy, University of Mississippi, MS 38677, USA*
[f] *Consejo de Investigaciones, Universidad Nacional de Rosario, Argentina*
[g] *Departamento de Química Orgánica, Facultad de Ciencias Bioquímicas y Farmacéuticas, Universidad Nacional de Rosario, Suipacha 531, S2002LRK, Rosario, Argentina*

† Electronic supplementary information (ESI) available. See DOI: 10.1039/d0md00291g

‡ These authors contributed equally to this work.

§ Present address: Department of Microbiology, Immunology & Pathology, Colorado State University, 1682 Campus Delivery, Fort Collins, CO 80523, USA.
¶ Present address: Department of Infectious Diseases, Division of Drug Discovery, Southern Research, Birmingham, AL 35205, USA.

This journal is © The Royal Society of Chemistry 2021

Published on 05 November 2020. Downloaded on 9/20/2023 4:42:31 PM.

interesting target to explore for the development of new antileishmanial drugs is the ortholog of the enzyme 2-*trans*-enoyl fatty acid reductase[3] from the *Mycobacterium tuberculosis* FASII complex. This enzyme, called InhA, was discovered as a target for the drug isoniazid (INH) (Fig. 1), which is one of the current drugs for the treatment of tuberculosis.[4] InhA catalyzes the reduction step that ends the process of a two carbon extension in the pathway of saturated fatty acid synthesis. Interestingly, antituberculosis drugs, such as triclosan (TRC) – an uncompetitive inhibitor of InhA – (Fig. 1), have also shown *in vitro* activity.[5] The kinetoplastid type II FAS is found in mitochondrial organelles.[6] Thus, since parasites have FASII enzymes they may be targeted by drugs active against bacterial fatty acid synthesis.

The *M. tuberculosis* FAS II complex is analogous to other bacterial FAS II, but is not capable of *de novo* fatty acid synthesis. However, FAS II from *Mycobacterium* is capable of elongating acyl-CoA generated by FAS I producing very long chain α-hydroxy, β-alkyl branched fatty acids known as mycolic acids. Even though mutations in the *inhA* gene are known to confer resistance to INH, the enzyme remains a validated and reliable target for drug discovery.

Triclosan[7] has been described as an InhA targeting antitubercular drug which does not require KatG activation; however, its poor bioavailability prevented its use.[8] In spite of that, TRC was used to inspire the development of other scaffolds such as 5-alkyl-diphenyl-ethers, one of which, 5-octyl-2-phenoxyphenol (8PP, Fig. 1),[9] has good antitubercular activity and higher solubility. Therefore, 8PP and similar molecules are good starting points for structure-based drug discovery.

One approach to enhance the activity of a drug candidate is to incorporate additional heterocycles as building blocks.[10] A recently introduced and popular strategy is to use 1,2,3-triazoles to link structurally diverse fragments with different pharmacophores.[11–13] A straightforward way to prepare 1,2,3-triazoles is the well-known click chemistry reaction which involves azides and alkynes as starting materials. This kind of approach is a very efficient way to build new compound libraries as drug candidates.[14] Also, when used as linkers, 1,2,3- triazoles are inert to degradation, soluble and prone to bind to biomolecular targets.[13]

Stec *et al.* have already taken advantage of this approach by preparing a collection of derivatives exchanging one of the TRC phenyl rings by 1,2,3-triazoles, introducing ketones, amides and isoxazoles.[15] One of those analogs with a 1,2,3-triazole on position 4′ and a butyl substituent in position 4 of the triazole showed micromolar activity against MTB and 98% inhibition of pure InhA (Fig. 1).

We have previously reported bioactive 1,2,3-triazolyl derivatives against *Leishmania* parasites (amino sterols) and *M. tuberculosis* (fatty acid derivatives).[16,17] In this opportunity, our aim was to develop novel structures based on the structures of TRC and 8PP, to find new chemical entities as candidates for antileishmanial drug discovery. The presence of putative enoyl-ACP reductase encoding genes in *Leishmania* prompted us to prepare and assay a library of 1,4 disubstituted 1,2,3-triazolyl catechols. The collection was initially assayed against *Leishmania donovani* promastigotes and *M. tuberculosis* H37Rv to determine IC_{50} and MIC. Cytotoxicity against Vero cells was also evaluated and afterwards, to understand the mechanism of action of these catechols and to test our hypothesis of an InhA ortholog being the target of these molecules, the most promising compounds were tested against purified Mtb InhA.

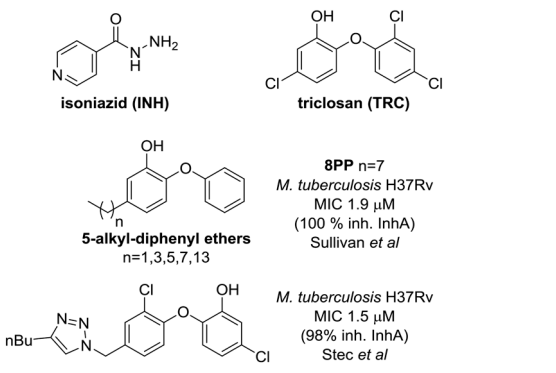

Fig. 1 Reported analogs with biological activity against *Mycobacterium tuberculosis*.

2. Results and discussion

2.1. Design and synthesis

The interactions between enoyl acyl ACP reductases (ENRs) and TRC (Fig. 1) have been characterized for *M. tuberculosis* InhA[18] as well as for *E. coli* FabI and *P. falciparum* (PfENR).[19] In the co-crystallized structure, TRC forms a complex with NAD^+ and InhA. The interactions of this ternary complex consist of the stacking of the hydroxylated ring with the nicotinamide ring of NAD^+. Other relevant interactions are the presence of hydrogen bonds of the hydroxy group of triclosan with the 2-hydroxy group of NAD^+ and with InhA Tyr158.[20] These interactions have proven to be the same for other ENR orthologs. Based on this knowledge, we hypothesized that a putative inhibitor of the *Leishmania* FABI ortholog should have a similar structure.

The search in the TDR Targets database[21] for enoyl-[acyl-carrier-protein] reductases (ENRs) provided an ORF for an InhA-like ortholog present in the *Leishmania major* genome (TDR Targets ID: 27659; GeneDB ID: LmjF.34.0610). Moreover, analysis of the *L. donovani* genome by Ravooru *et al.*[22] revealed that the E9B7Z4 encoded ORF is closely associated with the enzyme of the class *trans*-2-enoyl-CoA reductase (1.3.1.38), which was also well conserved along *Leishmania* spp. The activity of TRC against the intracellular and free form of *L. donovani* has been recently linked to ENRs by an *in silico* modelling based on the GenBank CBZ37546.1 sequence.[3] Based on these precedents we performed a multiple alignment of *M. tuberculosis*, *E. coli* ENRs and different *Leishmania* spp. putative ENR sequences. The result

Published on 05 November 2020. Downloaded on 9/20/2023 4:42:31 PM.

showed highly conserved residues on the substrate binding and active site loops. Also, as was shown before, putative ENR proteins of different *Leishmania* species were highly conserved (Fig. S1, ESI†). These precedents led us to design a collection of compounds based on TRC and 8PP that could potentially target leishmanial ENRs (Fig. 1).

As was previously mentioned, the 1,2,3-triazole motif is widely used in medicinal chemistry, being present in compounds with anticancer, anti-inflammatory, antituberculosis, antitrypanosomal, antibacterial and antiviral activities. Most of the reported bioactive 1,2,3-triazoles are exclusively 1,4-disubstituted, with little information on the results of expanding the chemical space by obtaining their 1,5-isomers.[23] Particularly, there are only a couple of examples of libraries of 1,4,5-trisubstituted 1,2,3-triazoles which have been assayed for antileishmanial or antituberculosis activity.[24] One of those libraries was composed of triazolopyridopyrimidines which have shown a moderate activity against different *Leishmania* species.[24]

Aiming to expand the SAR studies of the TRC scaffold, a new set of 1,2,3-triazolyl analogs was synthesized using thermal and Cu(I) catalyzed-cycloaddition (CuAAC) reactions. The CuAAC reaction is completely selective being extremely useful for the synthesis of 1,4-disubstituted-1,2,3-triazoles. The thermal cycloaddition provides a mixture of 1,5- and 1,4-regioisomers, being useful to expand our SAR studies (Scheme 1). Two series of 1,2,3-triazole analogs of TRC were proposed (Scheme 1, series 1). Due to the critical role of the TRC hydroxy group, the designed compounds contained this group in different scaffolds.[25] Additionally, the chlorine was removed since it is known that it diminishes the inhibitory activity and interferes with the bioavailability.[26] The series 1 scaffold has a phenol connected by a linker to a substituted 1,2,3-triazole that was introduced by a CuAAC reaction. In this series, the linker can be either a methyleneoxy group preserving the catechol moiety of TRC or a methylene group (Scheme 1, series 1). The methyl ether derivatives were also included for the sake of comparison with the free hydroxy derivatives.

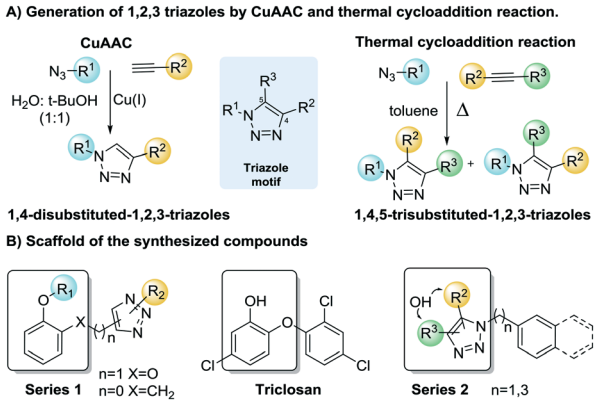

Scheme 1 1,4-Disubstituted- and 1,4,5-trisubstituted-1,2,3-triazoles generated by CuAAC reaction and thermal cycloaddition.

To increase the diversity of the collection expanding the explored chemical space, 1,4,5-trisubstituted-1,2,3-triazoles were also prepared (Scheme 1, series 2). These 1,4,5-trisubstituted-1,2,3-triazoles were prepared from different azides and internal alkynes by thermal cycloaddition, resulting in mixtures of isomers.

The synthesis started with the phenol etherification of catechol **1** and guaiacol **2** according to Williamson's reaction, producing the ether formation with propargyl bromide and potassium carbonate in methanol (Scheme 2). *O*-Propargyl-catechol **3** and *O*-propargyl-2-methoxyphenol **4** were obtained in 46% and 40% yield, respectively. The reaction with catechol **3** also provided the di-propargylated product in 13% yield as a by-product. In both reactions, some of the starting material was recovered and could be reused. Once the alkyne intermediates were obtained, the CuAAC reaction was performed with different azides containing aromatic and carbocyclic rings, and aliphatic, prenyl and alkyl ethyl ester chains (**5a–i**, **6a–e**, Scheme 2). The average yield for scaffold **5** was 74% and 77% for **6** (Table 1).

The other members of series 1 were prepared with salicyl azide **8**. This key intermediate was prepared from commercially available salicyl alcohol **7** by reaction with sodium azide and triphenylphosphine and in DMF and carbon tetrachloride.[27] The CuAAC reaction was performed with commercially available terminal alkynes. The alkynes used were 1-propyne, 1-pentyne, 1-octyne, ethynylbenzene and pent-4-yn-1-ylbenzene (Scheme 2). The average yield of the reaction was 65% (Table 1).

Finally, a thermal cycloaddition reaction in toluene was used to prepare series 2 with the aim of mimicking the phenol aromatic ring by a hydroxylated triazole motif. Three different azides and three internal alkynes were employed obtaining a mixture of 1,4,5-substituted-1,2,3-triazoles. Benzyl azide **10**, 3-phenylpropyl azide **12** and 2-(azidomethyl) naphthalene **14** were combined with the internal alkynes oct-2-yn-1-ol, 3-phenylprop-2-yn-1-ol, and hex-3-yn-2-ol to afford the products **11**, **13** and **15** (Scheme 3). Phenylpropyl azide **12**, with a longer linker, is more flexible than benzyl azide **10**, and the naphthyl derivative is bulkier and has an extended pi-stacking surface.

The yields were calculated including both isolated isomers, which were obtained as a 1 : 1 mixture of both

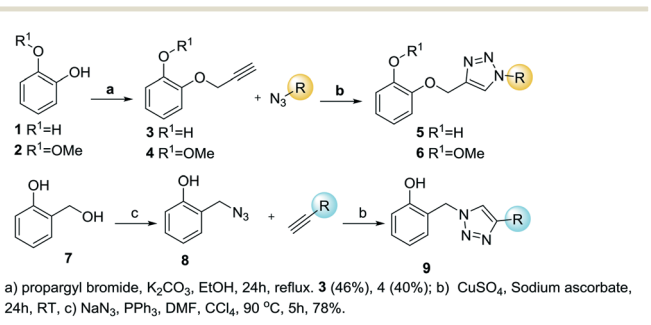

Scheme 2 Synthesis of products starting from catechol **1**, 2-methoxyphenol **2** and salicyl alcohol **7**.

This journal is © The Royal Society of Chemistry 2021

Published on 05 November 2020. Downloaded on 9/20/2023 4:42:31 PM.

Table 1 Synthesized 1,2,3-triazoles derived from catechol, 2-methoxyphenol and salicyl azide

Comp.	Yield (%)	R	Comp.	Yield (%)	R
5a	76	CH_2Ph	**6a**	70	CH_2Ph
5b	81	$(CH_2)_3Ph$	**6b**	82	$(CH_2)_3Ph$
5c	71	Cinnamyl	**6c**	73	Cyclohexyl
5d	68	Cyclohexyl	**6d**	79	C_8H_{17}
5e	65	C_8H_{17}	**6e**	80	$(CH_2)COOEt$
5f	82	$C_{13}H_{27}$	**9a**	76	C_3H_7
5gZ	70	Neryl	**9b**	81	C_5H_{11}
5gE	70	Geranyl	**9c**	71	C_8H_{17}
5h	79	$(CH_2)COOEt$	**9d**	68	Ph
5i	78	$(CH_2)_4COOEt$	**9e**	65	$(CH_2)_2Ph$

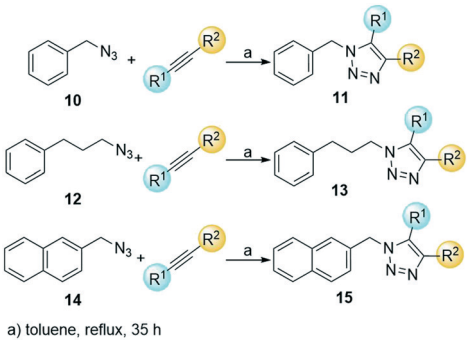

Scheme 3 Synthesis of the products using the thermal cycloaddition methodology.

regioisomers. The ratio was calculated by ^1H NMR. The average yield for each scaffold was 61%, 51% and 77% for triazoles **11a–e**, **13a–f** and **15a–f**, respectively (Table 2).

The collection of 37 triazolyl TRC analogs were characterized using ^1H and ^{13}C NMR and mass spectrometry. The regiochemistry of the series 2 products was determined using nuclear Overhauser effect (NOE) experiments.

For example, for product **11a** the signal of the methylene of the methylenehydroxy group at 4.53 ppm showed a NOE with the signal of the methylene of the benzyl group at 5.59 ppm and with the methylene from the pentyl group at 2.56 ppm (Fig. 2). For isomer **11b**, irradiation on the same methylene only showed a NOE with the methylene of the pentyl chain (Fig. 2).

Table 2 Synthesized 1,2,3-triazoles using thermal cycloaddition

Comp	R^1	R^2	Comp	R^1	R^2	Yld (%)
11a	CH_2OH	C_5H_{11}	**11b**	C_5H_{11}	CH_2OH	52
			11c	Ph	CH_2OH	76
11d	$CH(OH)CH_3$	C_2H_5	**11e**	C_2H_5	$CH(OH)CH_3$	56
13a	CH_2OH	C_5H_{11}	**13b**	C_5H_{11}	CH_2OH	46
13c	CH_2OH	Ph	**13d**	Ph	CH_2OH	66
13e	$CH(OH)CH_3$	C_2H_5	**13f**	C_2H_5	$CH(OH)CH_3$	42
15a	CH_2OH	C_5H_{11}	**15b**	C_5H_{11}	CH_2OH	69
15c	CH_2OH	Ph	**15d**	Ph	CH_2OH	94
15e	$CH(OH)CH_3$	C_2H_5	**15f**	C_2H_5	$CH(OH)CH_3$	75

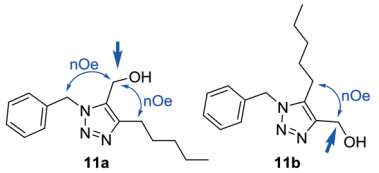

Fig. 2 NOE experiments of **11a** and **11b**.

2.2. Biology

The final obtained compounds were assayed for biological activity against *L. donovani* promastigotes, against *M. tuberculosis* H37Rv *in vitro* (since the prepared library has been designed based on compounds with proven antimycobacterial activity) and against mammalian Vero cell lines, for cytotoxicity evaluation (Table 3). Most of the compounds did not present activity against *L. donovani* promastigotes at 60 μM, the maximum concentration tested. None of the compounds showed cytotoxicity against Vero cells at the maximum concentration tested of 20 μM. Pentamidine and amphotericin B were used as controls, with IC_{50} of 4.40 μM and 0.11 μM, respectively. For *M. tuberculosis* the minimal inhibitory concentration (MIC) was determined by a serial microdilution colorimetric assay using MTT as a viability indicator.[28] In this case TRC was used as a positive control, with a MIC_{99} of 43.0 μM.[9]

Only four compounds of the series showed IC_{50} below 60 μM against *L. donovani*, with **5f** being the most active compound showing an IC_{50} of 13.4 μM (Table 3). Regarding the *M. tuberculosis* assays, the results showed that only analogs **9a**, **9b** and **9d** have MIC below 100 μM. These 3 compounds belong to series 1 and have MIC of 20.0 μM (Table 3).

Having completed the screening stage, the next step was validating the target of the compounds. To do this, the most promising analogs were assayed on the purified mycobacterial InhA.[19]

The initial assay was performed at a fixed compound concentration, 40 μM for derivatives **5f**, **5gZ**, and **5gE** and 50 μM for derivatives **9a**, **9b**, **9d** and **15b**. The reaction velocity in the absence $(v)_0$ and presence of the inhibitor $(v)_I$ was determined. The results were disappointing since the tested compounds proved to be extremely poor in inhibitory efficacy with only marginal inhibition shown by 3 of the most promising compounds compared to TRC which showed an IC_{50} of 1.0 μM.[9] The remaining enzyme activities were 63, 85 and 92% for compounds **5f**, **5gZ** and **9a**, respectively (Table 3).

When discussing the most active compounds against *L. donovani*, the disappointing results could be explained with the fact that they were assayed on the mycobacterial enzyme and not on the actual *L. donovani* orthologue. There are substantial differences between *Leishmania* spp. and *M. tuberculosis* fatty acid synthesis end products. While the parasite fatty acids are composed of C14 to C22 fatty acids,[29] the mycobacterial FASII could elongate fatty acids up to ~40 carbons.[30] These

Table 3 Results of enzyme inhibition, MICs and cytotoxicity for active compounds against *L. donovani* and *M. tuberculosis*

Comp	*Ld*[a] IC_{50} (μM)	*Mt* H37Rv[b] MIC (μM)	Vero IC_{50} (μM)	*Mt* InhA[c] inh (%)
5f	13.4	>100	>20	63
5gZ	55.0	>100	>20	85
5gE	51.9	>100	>20	N.I.
9a	>60	20.0	>20	92
9b	>60	20.0	>20	N.I.[d]
9d	>60	20.0	>20	N.I.
15b	31.4	>100	>20	N.I.
TRC		43.0		
PM	4.40			
AMB	0.11			

TRC = triclosan, PM = pentamidine, AMB = amphotericin B.[a] *Ld*: *L. donovani* promastigotes, evaluated by the Alamar blue assay. [b] *Mt* H37Rv: *Mycobacterium tuberculosis* H37Rv, evaluated by a serial microdilution colorimetric assay using MTT as a viability indicator. [c] *Mt* InhA: remaining *M. tuberculosis* InhA activity. [d] N.I.: no inhibition.

Published on 05 November 2020. Downloaded on 9/20/2023 4:42:31 PM.

variations would probably justify the sequence differences between the *M. tuberculosis* and *Leishmania* spp. ENRs that will ultimately may result in the lack of inhibition of InhA. Consequently, we should explore this in detail to obtain a definitive conclusion of whether minor but structurally important differences between the different ENRs may condition the inhibitory activity.

Also, there is low or null inhibition of the most promising compounds against *M. tuberculosis*. The compounds that display some activity, analogs **5f**, **5gZ** and **9a**, share the critical phenolic hydroxyl on their structure with TRC and 8PP (Table 3), nevertheless they did not show an inhibitory effect on InhA. Those results could be explained by the presence of different target/s, a hypothesis that could be further investigated.

2.3. Structure–activity relationship (SAR)

In the previous section, the results of the biological activities against *L. donovani* and *M. tuberculosis* were presented with only a few compounds displaying against each pathogen. The inhibition capacity towards *M. tuberculosis* InhA of the most attractive collection members was assayed, resulting in surprisingly poor inhibition. As was previously discussed, there is a lack of overlap between the compounds which show greater potency for *L. donovani* and those which show the most potency for *M. tuberculosis*. This contrast becomes more visible when analyzing the heatmap in Fig. 3 which clearly shows the leads for each pathogen in a brighter tone of blue. Therefore, the need for a more profound analysis of the structure–activity relationship for both *L. donovani* and *M. tuberculosis* separately became stronger.

As regards *L. donovani* promastigotes, two populations of active compounds were identified. The first group comprises analogs from series 1 (**5f**, **5gZ**, **5gE**; IC_{50} = 13.4, 55.0 and 51.9 μM respectively); while the second consists of only compound **15b** (IC_{50} = 31.4 μM) from series 2 (Fig. 4). The active compounds contain long lipophilic substituents on the triazole (pentyl, octyl, geranyl, neryl and tridecyl) and their activity seems to be related to a triazole side chain longer than 5 carbons. The restricted conformation produced by the double-bond on the isoprenyl derivatives seems to be detrimental to the activity. Comparison of analogs **15b** and **5f** clearly showed that the longer aliphatic saturated chain improved the activity. This structural feature resembles the 5-alkyl-diphenyl ether moiety present in 8PP where the saturated lipophilic chain plays a critical role in the binding to InhA.[9] Three out of the four active compounds have a phenol in their structure, and the fourth compound has a methylenehydroxy group attached to the triazole. None of the methylated phenol derivatives was active, demonstrating the importance of the hydroxy group in the activity. The fact that three active compounds are from series 1 confirms that the incorporation of the ether on the structure mimics TRC and 8PP.

On the other hand, the results on *M. tuberculosis* show that compounds **9a** and **9b** have a lipophilic saturated aliphatic chain on the 1,2,3-triazole (Fig. 5) being like 8PP, but notably less active (8PP MIC_{99} = 6.4 μM). The other active analog is **9d**, which has a phenyl ring decorating the 1,2,3-triazole, a fact that shows that the flexible lipophilic chain

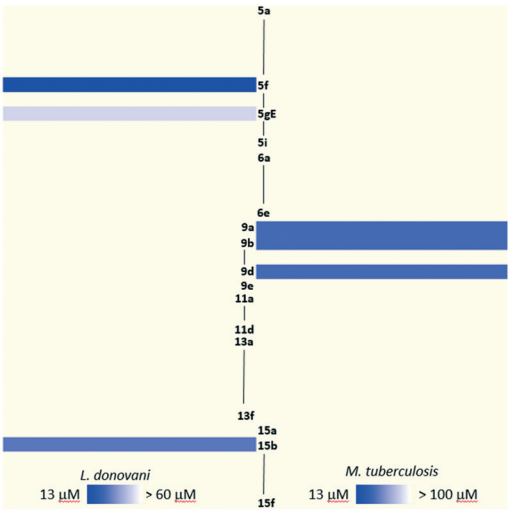

Fig. 3 Heatmap of active compounds against *L. donovani* and *M. tuberculosis*.

This journal is © The Royal Society of Chemistry 2021

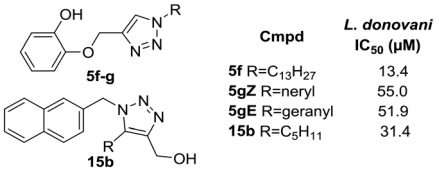

Cmpd	*L. donovani* IC_{50} (μM)
5f R=$C_{13}H_{27}$	13.4
5gZ R=neryl	55.0
5gE R=geranyl	51.9
15b R=C_5H_{11}	31.4

Fig. 4 Active compounds against *L. donovani* promastigotes.

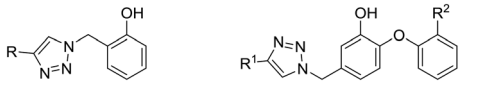

M. tuberculosis H37Rv MIC (μM)		*M. tuberculosis* H37Rv MIC (μg/mL - μM)	
9a R=C_3H_7	20.0	**PT510** R^1=Et R^2=CN	0.625 / 2.02
9b R=C_5H_{11}	20.0	**PT509** R^1=Et R^2=Me	1.25 / 3.90
9d R=Ph	20.0	**PT163** R^1=Ph R^2=Me	3.95 / 11.1
Triclosan	43.0		

Fig. 5 Active compounds against *M. tuberculosis* H37Rv (MIC).

Published on 05 November 2020. Downloaded on 9/20/2023 4:42:31 PM.

can be replaced by that non-polar bulkier ring. Surprisingly, derivative **9c** that holds an octyl chain, the derivative that is structurally the most closely related to 8PP, was inactive. The activity *vs.* aliphatic tail relationship for the C5 derivative is less significant than for the C8 derivative when comparing the diphenyl ethers.[9] Ethers **5e** and **6d**, which also resemble 8PP, were also inactive. The rest of the library does not show activity against *M. tuberculosis* H37Rv with MICs higher than 32 μM. These compounds are considerably less active than the previous collection based on 8PP reported by our group, which reached low micromolar MIC on H37Rv.[16,31] Nevertheless, the active members of the collection are twice more active than TRC that has a MIC of 43.0 μM.

A close comparison with the triazolyl-diphenyl ethers reported by Spagnuolo *et al.*[32] showed that not only the substitution pattern on the phenol ring, but mostly the presence of the phenoxy moiety, plays a critical role in the antitubercular activity (Fig. 5). This is clearly seen for compounds **9a**, **9b**, and **9d** that are 1.8, 5.1 and 9.9 times less active than the diphenyl ethers **PT163**, **PT509** and **PT510**, respectively (Fig. 5).

2.4. Physicochemical parameters

Finally, the physicochemical parameters were calculated *in silico* for the active compounds of the library using Data Warrior software[33] (Fig. S2, ESI†). The parameters of Lipinski's rule of five were calculated, including the topological polar surface area (TPSA).

Lipinski's rule of five is widely used for determination of good pharmacokinetic properties. The parameters considered were the molecular weight (MW $<$ 500 Da), the partition coefficient between water and octanol ($0 < \log P < 5$) and the number of hydrogen bond acceptors (nNHOH $<$ 10) and donors (nON $<$ 5). If there were two or more violations of these rules, the compounds would present poor oral administration, but there are exceptions to these rules. Another useful parameter is the topological polar surface area (TPSA) that considers the electron density distribution in the molecule and gives us an idea of the capacity to penetrate biological membranes. This parameter is commonly used to establish if the compounds could penetrate the blood brain barrier. All the active compounds comply with the rule of five and TPSA parameters. Only compound **5f** violates one rule having a $\log P$ of 5.67. Interestingly, this compound is the most active in the collection against *L. donovani* promastigotes. This result is not discouraging since the physicochemical requirements could be taken in a lighter way in order to obtain antiparasitic lead compounds susceptible of further improvement.[34]

3. Experimental

3.1. Synthesis

General procedure for the synthesis of 1,4-disubstituted 1,2,3-triazoles. Alkyne (1 eq.) and azide (1.5 eq.) were suspended in 4 mL of ^{t}BuOH : H_2O (1 : 1). Afterwards, aqueous 1 M $CuSO_4$ (0.025 eq.) solution and aqueous 1 M sodium ascorbate (0.1 eq.) solution were added. The mixture was stirred overnight at room temperature. Brine was added and the solution was extracted with dichloromethane. Combined organic extracts were dried with sodium sulphate and evaporated. The resulting residue was purified by column chromatography over silica gel using an increasing AcOEt/hexane gradient to afford desired pure products.

*Synthesis of 2-((1-tridecyl-1H-1,2,3-triazol-4-yl)methoxy) phenol (**5f**).* Colorless oil. ^{1}H NMR (300 MHz, $CDCl_3$) δ: 7.54 (s, 1H); 7.00 (dd, J_1 = 7.8 Hz, J_2 = 1.5 Hz, 1H); 6.94 (dd, J_1 = 7.8 Hz, J_2 = 2.1 Hz, 1H); 6.90 (dd, J_1 = 7.9 Hz, J_2 = 1.5 Hz, 1H); 6.82 (ddd, J_1 = 7.8 Hz, J_2 = 2.5 Hz, J_3 = 2.3 Hz, 1H); 6.11 (s, 1H); 5.26 (s, 2H); 4.35 (t, J = 7.9 Hz, 2H); 1.09 (q, J = 7.6 Hz, 2H); 1.35–1.22 (m, 20H); 0.88 (t, J = 6.7 Hz, 3H). ^{13}C NMR (75 MHz, $CDCl_3$) δ: 146.6 (C); 145.7 (C); 143.5 (C); 122.6 (CH); 122.5 (CH); 120.1 (CH); 115.6 (CH); 113.8 (CH); 63.2 (CH_2); 50.5 (CH_2); 31.9 (CH_2); 30.2 (CH_2); 29.6 (CH_2); 29.5 (CH_2); 29.4 (CH_2); 29.3 (CH_2); 29.0 (CH_2); 26.4 (CH_2); 22.7 (CH_2); 14.1 (CH_3).

*Synthesis of 4-((2-methoxyphenoxy)methyl)-1-octyl-1H-1,2,3-triazole (**6d**).* Colourless oil. ^{1}H NMR (300 MHz, $CDCl_3$) δ: 7.61 (s, 1H); 7.04 (dd, J_1 = 7.0 Hz, J_2 = 2.2 Hz, 1H); 6.94 (m, 1H); 6.90 (s, 1H); 6.89 (dd, J_1 = 7.7 Hz, J_2 = 2.5 Hz, 1H); 5.30 (s, 2H); 4.32 (t, J = 7.3 Hz, 2H); 3.87 (s, 3H); 1.88 (q, J = 6.0 Hz, 2H); 1.37–1.20 (m, 10H); 0.87 (t, J = 6.0 Hz, 3H). ^{13}C NMR (75 MHz, $CDCl_3$) δ: 149.6 (C); 147.6 (C); 144.3 (C); 122.6 (CH); 121.8 (CH); 120.9 (CH); 114.4 (CH); 111.8 (CH); 63.3 (CH_2); 55.9 (CH_3) 50.4 (CH_2); 31.7 (CH_2); 30.2 (CH_2); 29.0 (CH_2); 28.9 (CH_2); 26.4 (CH_2); 22.6 (CH_2); 14.0 (CH_3).

*Synthesis of 2-((4-pentyl-1H-1,2,3-triazol-1-yl)methyl)phenol (**9b**).* White solid. Mp: 88.2–89.2 °C. ^{1}H NMR (300 MHz, $CDCl_3$) δ: 7.45 (s, 1H), 7.24 (s, 1H), 7.19 (d, J = 7.8 Hz, 1H), 7.01 (d, J = 7.8 Hz, 1H), 6.86 (t, J = 7.3 Hz, 1H), 5.52 (s, 2H), 2.67 (t, J = 7.7 Hz, 2H), 1.63 (p, J = 7.5 Hz, 2H), 1.36–1.34 (m, 4H), 0.85 (t, J = 6.8 Hz, 3H). ^{13}C NMR (75 MHz, $CDCl_3$) δ: 155.4 (C), 148.4 (C), 130.4 (CH), 130.4 (CH), 121.6 (CH), 121.5

Published on 05 November 2020. Downloaded on 9/20/2023 4:42:31 PM.

(C), 120.3 (CH), 116.9 (CH), 49.8 (CH_2), 31.4 (CH_2), 29.0 (CH_2), 25.5 (CH_2), 22.3 (CH_2), 13.9 (CH_3). ESI-HRMS calcd. for ($M + H^+$) $C_{14}H_{19}N_3O$ 246.1606, found 246.1601.

General procedure for the synthesis of 1,2,3-triazoles by thermal cycloaddition. Alkyne (1 eq.) and azide (1 eq.) were suspended in 2 mL per eq. of toluene. The mixture was stirred and heated under reflux for 35 hours. Then, it was cooled down to room temperature it was cooled down to room temperature, brine was added, and the solution was extracted with dichloromethane. Combined organic extracts were dried with sodium sulphate and evaporated. The resulting residue was purified by column chromatography over silica gel using an increasing AcOEt/hexane gradient to afford desired pure products.

*Synthesis of (1-benzyl-4-pentyl-1H-1,2,3-triazol-5-yl)methanol (**11a**).* White solid. MP: 59.3–60.0 °C. ^{1}H NMR (300 MHz, $CDCl_3$) δ: 7.29–7.30 (m, 3H); 7.22–7.19 (m, 2H); 5.59 (s, 2H); 4.53 (d, J = 4.7 Hz, 2H); 2.56 (t, J = 7.7 Hz, 2H); 1.60 (p, J = 7.0 Hz, 2H); 1.27 (m, 4H); 0.85 (t, J = 6.5 Hz, 3H). ^{13}C NMR (75 MHz, $CDCl_3$) δ: 146.5 (C); 135.2 (C); 131.9 (C); 128.9 (CH); 128.3 (CH); 127.5 (CH); 52.3 (CH_2); 52.1 (CH_2); 31.5 (CH_2); 29.6 (CH_2); 26.8 (CH_2); 22.4 (CH_2); 14.0 (CH_3). ESI-HRMS calcd. for ($M + H^+$) $C_{15}H_{21}N_3O$ 260.1763; found 260.1757.

*Synthesis of (4-pentyl-1-(3-phenylpropyl)-1H-1,2,3-triazol-5-yl) methanol (**13a**).* Colorless oil. ^{1}H NMR (300 MHz, $CDCl_3$) δ: 7.31–7.17 (m, 5H); 4.62 (d, J = 4.3 Hz, 2H); 4.36 (t, J = 7.3 Hz, 2H); 2.69 (t, J = 7.3 Hz, 2H); 2.61 (t, J = 7.6 Hz, 2H); 2.29 (q, J = 7.1 Hz, 2H); 1.68–1.62 (m, 2H); 1.31 (m, 4H, C7–H); 0.88 (t, J = 7.0 Hz, 3H). ^{13}C NMR (75 MHz, $CDCl_3$) δ: 146.1 (C); 140.6 (C); 131.3 (C); 128.5 (CH); 128.4 (CH); 126.2 (CH); 52.3 (CH_2); 47.9 (CH_2); 32.7 (CH_2); 31.5 (CH_2); 31.4 (CH_2); 29.7 (CH_2); 24.9 (CH_2); 22.4 (CH_2); 14.0 (CH_3). ESI-HRMS calcd. for ($M + H^+$) $C_{17}H_{26}N_3O$ 288.2076; found 288.2070.

*Synthesis of (1-(naphthalen-2-ylmethyl)-5-pentyl-1H-1,2,3-triazol-4-yl)methanol (**15b**).* White solid. MP: 79.2–80.2 °C. ^{1}H NMR (300 MHz, $CDCl_3$) δ: 7.80 (m, 3H); 7.76 (s, 1H); 7.50–7.47 (m, 2H); 7.27 (m, 1H); 5.64 (s, 2H); 4.72 (d, J = 5.4 Hz, 2H); 2.59 (t, J = 7.5 Hz, 2H); 1.34 (p, J = 7.5 Hz, 2H); 1.14–1.12 (m, 4H); 0.72 (t, J = 7.0 Hz, 3H). ^{13}C NMR (75 MHz, $CDCl_3$) δ: 144.9 (C); 135.2 (C); 133.2 (C); 133.0 (C); 132.4 (C); 129.0 (CH); 127.8 (CH); 127.8 (CH); 126.6 (CH); 126.5 (CH); 126.2 (CH); 124.7 (CH); 55.9 (CH_2); 52.2 (CH_2); 31.4 (CH_2); 28.5 (CH_2); 22.6 (CH_2); 22.1 (CH_2); 13.7 (CH_3). ESI-HRMS calcd. for ($M + H^+$) $C_{19}H_{24}N_3O$ 310.1841; found 310.1904.

3.2. Biology

Bacterial strain *M. tuberculosis* H37Rv. *M. tuberculosis* strain H37Rv (kindly provided by Dr. L. Barrera, Instituto Nacional de Microbiología "C. G. Malbrán", Argentina) was routinely grown at 37 °C under gentle agitation in Middlebrook 7H9 broth (Difco Laboratories, Detroit, MI, USA) supplemented with 1/10 v/v of ADS (50 g L^{-1} BSA fraction V, 20 g L^{-1} dextrose and 8.1 g L^{-1} NaCl) and glycerol (1% w/v). Tween 80 was added to prevent clumping (0.05% w/v). This medium was designated as 7H9-ADS-Gly for short. When needed, solid medium Middlebrook 7H11 supplemented with ADS (1/10 v/v) and glycerol (1% v/v) was used.

***In vitro* activity against *M. tuberculosis* H37Rv.** Stock solutions for all the tested compounds were made in DMSO at 40 mM. Working solutions were made by dilution in the above described 7H9-ADS-G medium at a final concentration of 400 μM. Antimycobacterial activity was determined by two-fold dilution of the compounds in Middlebrook 7H9-ADS-Gly medium as described previously.[16] For this purpose, 96-well plates (Falcon, Cat number 3072, Becton Dickinson, Lincoln Park, NJ) were used. The 96 well-plates received 100 μL of Middlebrook 7H9 broth and a serial two-fold dilution of the compounds was made directly on the plate. The initial and final drug concentrations tested were 20 μM and 1.25 μM, respectively. The compounds were tested in three biological repetitions each one in technical duplicate. Rifampicin (final concentrations ranging from 2 mg mL^{-1} to 0.16 mg mL^{-1}; stock solution prepared as a 10 mg mL^{-1} solution in methanol) was used as a control drug. The inoculum was prepared as a 1/25 dilution of a fresh mid-log *M. tuberculosis* H37Rv suspension (O.D equivalent to Mc Farland 1.0 scale value) made in Middlebrook 7H9-ADS-G. A 100 μL aliquot (containing approximately 10^6 colony forming units) was used to inoculate the wells. The plates were sealed with Parafilm and incubated at 37 °C for five days. After visual inspection of the plates, the turbidity was recorded and the final value for the MIC was assessed by addition of 30 μL of a stock MTT solution as described elsewhere.[35] The minimum inhibitory concentration (MIC) was defined as the lowest drug concentration preventing mycobacterial growth (yellow color = growth inhibition).

InhA inhibition assay. The InhA inhibition activity was tested using *trans*-2-dodecenoyl-coenzyme A (DD-CoA) and wild-type InhA as described previously.[36] Reactions were initiated by the addition of 100 nM InhA to solutions containing 25 μM DD-CoA, 40–50 μM inhibitor, and 250 μM NADH in 30 mM PIPES and 150 mM NaCl, pH 6.8 buffer. Control reactions were carried out under the same conditions as described above but without an inhibitor. The inhibitory activity of each derivative was expressed as the percentage inhibition of InhA activity (initial velocity of the reaction) with respect to the control reaction without an inhibitor.

***In vitro* antileishmanial assay.** *Leishmania donovani* promastigotes of the S1 Sudan strain (2×10^6 cells per mL) were cultured at 26 °C in plastic flasks (25 cm^2) containing RPMI-1640 medium (without sodium bicarbonate and sodium pyruvate) with 10% FBS. *L. donovani* promastigotes were subcultured twice a week, with the highest cell concentration in the range of 20–25 × 10^6 promastigotes per mL. Compounds with appropriate dilution were added to a 96 well microplate with promastigotes (2×10^6 cells per mL) reaching final concentrations of 40, 8 and 1.6 μg mL^{-1}. The plates were incubated at 26 °C for 72 h and the growth was determined by the Alamar blue assay.[37] pentamidine and amphotericin B were used as standard antileishmanial agents. IC_{50} values were obtained by non-linear regression of

 This journal is © The Royal Society of Chemistry 2021

Published on 05 November 2020. Downloaded on 9/20/2023 4:42:31 PM.

dose response logistic functions, using the Microsoft Excel-based plug-in XLfit. All experiments were performed in triplicate.

Cytotoxicity assay. The *in vitro* cytotoxicity was determined against mammalian kidney fibroblasts (VERO). Vero cells (African green monkey kidney) were cultured in MEM medium supplemented with 10% heat inactivated FCS, 0.15% (w/v) $NaHCO_3$, 100 U mL^{-1} penicillin and 100 U mL^{-1} streptomycin at 37 °C in a 5% CO_2 atmosphere.

The assay was performed in 96-well tissue culture-treated plates as described earlier.[38] The cells were seeded to the wells of the plate (25 000 cells per well) and incubated for 24 h. Samples were added and the plates were again incubated for 48 h. The number of viable cells was determined by the neutral red assay. IC_{50} values were determined from logarithmic graphs of growth inhibition *versus* concentration. Doxorubicin was used as a positive control (IC_{50} = 14 mM, Vero cells), while DMSO was used as a vehicle control.

4. Conclusions

For the present study, a collection of thirty-seven 1,4-disubstituted and 1,4,5-trisubstituted 1,2,3-triazole analogs of triclosan were designed based on the structure of reported InhA inhibitors. The 1,4-disubstituted products were prepared using CuAAC, while for the 1,4,5-trisubstituted derivatives, thermal cycloaddition was used, with both cases achieving good yields. The preparation of 1,4,5-trisubstituted 1,2,3-triazoles has not been exploited in library preparation, in part due to the lack of selectivity. In our approach this fact proved to be a valuable tool to diversify our collection and expand the chemical space explored. The collection was initially assayed against *L. donovani* and *M. tuberculosis*. For *L. donovani*, four compounds have IC_{50} below 60 μM. The activity profile showed that a lipophilic substituent in the triazole and an alcohol were required for activity. When the collection was assayed *in vitro* against *M. tuberculosis* H37Rv, 3 derivatives displayed a MIC_{99} of 20.0 μM. To validate the original hypothesis that the compounds have the InhA *L. donovani* ortholog as the target, the most promising compounds of the library were assayed on the mycobacterial enzyme, showing poor inhibition. These results suggested that InhA may not be the main target for the active compounds against *M. tuberculosis*. Nevertheless, to effectively discard the hypothesis for the active compounds against *L. donovani*, the compounds should be tested on the leishmanial enzyme.

In summary, compound **5f** could be considered a valuable starting point for future antileishmanial drug development, based on its simple preparation and promising activity. The possibility that the activity could be linked to a putative leishmanial InhA orthologue should be a matter of future investigation, together with the exploration of new structural modifications to enhance the activity. For this purpose, the purification of the putative *Leishmania* ORF and its assay for ENR activity would lead the priority list. This will be followed by testing the analogues against this potential InhA orthologue. In parallel, the most promising candidates will be assayed against other *Leishmania* species including the intracellular stage of the parasite.

Conflicts of interest

There are no conflicts to declare.

Acknowledgements

This work was supported in part by grants from the National Research Council of Argentina, CONICET (PIP 2012-14/0448); Agencia Nacional de Promoción Científica y Tecnológica, ANPCyT-Argentina (PICT 2011/0589 to GRL and PICT 2005/38198 to HRM); National Institutes of Health, NIH (GM102864 to PJT); Universidad Nacional de Rosario (BIO503 to GRL) and Fundación Josefina Prats. The research leading to these results has, in part, received funding from the UK Research and Innovation *via* the Global Challenges Research Fund under grant agreement 'A Global Network for Neglected Tropical Diseases' grant number MR/P027989/1. GRL is a member of the scientific staff of CONICET-Argentina. HRM is a career member of CIUNR-Argentina. D. G. G., J. F. de L. and A. I. R. B. thanks CONICET for the award of a Fellowship.

Notes and references

1 WHO, Leishmaniasis report, World Health Organization, 2019.
2 J. Yao and C. O. Rock, *Biochim. Biophys. Acta, Mol. Cell Biol. Lipids*, 2017, **1862**, 1300–1309.
3 S. Yadav, H. Mandal, V. Saravanan, P. Das and S. K. Singh, *J. Biomol. Struct. Dyn.*, 2020, 1–14.
4 C. E. Barry, D. C. Crick and M. R. McNeil, *Infect. Disord.: Drug Targets*, 2007, **7**, 182–202.
5 V. Arango, J. J. Domínguez, W. Cardona, S. M. Robledo, D. L. Muñoz, B. Figadere and J. Sáez, *Med. Chem. Res.*, 2012, **21**, 3445–3454.
6 K. S. Paul, C. J. Bacchi and P. T. Englund, *Eukaryotic Cell*, 2004, **3**, 855–861.
7 L. M. McMurry, P. F. McDermott and S. B. Levy, *Antimicrob. Agents Chemother.*, 1999, **43**, 711–713.
8 L. Q. Wang, C. N. Falany and M. O. James, *Drug Metab. Dispos.*, 2004, **32**, 1162–1169.
9 T. J. Sullivan, J. J. Truglio, M. E. Boyne, P. Novichenok, X. Zhang, C. F. Stratton, H. J. Li, T. Kaur, A. Amin, F. Johnson, R. A. Slayden, C. Kisker and P. J. Tonge, *ACS Chem. Biol.*, 2006, **1**, 43–53.
10 A. N. Bootsma and S. E. Wheeler, *ChemMedChem*, 2018, **13**, 835–841.
11 A. Çapcı, M. M. Lorion, H. Wang, N. Simon, M. Leidenberger, M. C. Borges Silva, D. R. M. Moreira, Y. Zhu, Y. Meng, J. Y. Chen, Y. M. Lee, O. Friedrich, B. Kappes, J. Wang, L. Ackermann and S. B. Tsogoeva, *Angew. Chem., Int. Ed.*, 2019, **58**, 13066–13079.

Published on 05 November 2020. Downloaded on 9/20/2023 4:42:31 PM.

12 V. B. Sokolov, A. Y. Aksinenko, T. A. Epishina and T. V. Goreva, *Russ. Chem. Bull.*, 2019, **68**, 1424–1428.
13 K. Bozorov, J. Zhao and H. A. Aisa, *Bioorg. Med. Chem.*, 2019, **27**, 3511–3531.
14 P. Thirumurugan, D. Matosiuk and K. Jozwiak, *Chem. Rev.*, 2013, **113**, 4905–4979.
15 J. Stec, C. Vilcheze, S. Lun, A. L. Perryman, X. Wang, J. S. Freundlich, W. Bishai, W. R. Jacobs, Jr. and A. P. Kozikowski, *ChemMedChem*, 2014, **9**, 2528–2537.
16 D. G. Ghiano, A. de la Iglesia, N. Liu, P. J. Tonge, H. R. Morbidoni and G. R. Labadie, *Eur. J. Med. Chem.*, 2017, **125**, 842–852.
17 E. O. Porta, P. B. Carvalho, M. A. Avery, B. L. Tekwani and G. R. Labadie, *Steroids*, 2014, **79**, 28–36.
18 M. R. Kuo, H. R. Morbidoni, D. Alland, S. F. Sneddon, B. B. Gourlie, M. M. Staveski, M. Leonard, J. S. Gregory, A. D. Janjigian, C. Yee, J. M. Musser, B. Kreiswirth, H. Iwamoto, R. Perozzo, W. R. Jacobs, J. C. Sacchettini and D. A. Fidock, *J. Biol. Chem.*, 2003, **278**, 20851–20859.
19 J. S. Freundlich, F. Wang, C. Vilchèze, G. Gulten, R. Langley, G. A. Schiehser, D. P. Jacobus, W. R. Jacobs Jr. and J. C. Sacchettini, *ChemMedChem*, 2009, **4**, 241–248.
20 T. J. Sullivan, J. J. Truglio, M. E. Boyne, P. Novichenok, X. Zhang, C. F. Stratton, H.-J. Li, T. Kaur, A. Amin, F. Johnson, R. A. Slayden, C. Kisker and P. J. Tonge, *ACS Chem. Biol.*, 2006, **1**, 43–53.
21 L. Urán Landaburu, A. J. Berenstein, S. Videla, P. Maru, D. Shanmugam, A. Chernomoretz and F. Agüero, *Nucleic Acids Res.*, 2019, **48**, D992–D1005.
22 N. Ravooru, S. Ganji, N. Sathyanarayanan and H. G. Nagendra, *Front. Genet.*, 2014, **5**, 291.
23 D. Dheer, V. Singh and R. Shankar, *Bioorg. Chem.*, 2017, **71**, 30–54.
24 R. Adam, P. Bilbao-Ramos, B. Abarca, R. Ballesteros, M. E. González-Rosende, M. A. Dea-Ayuela, F. Estevan and G. Alzuet-Piña, *Org. Biomol. Chem.*, 2015, **13**, 4903–4917.
25 A. Chollet, L. Maveyraud, C. Lherbet and V. Bernardes-Génisson, *Eur. J. Med. Chem.*, 2018, **146**, 318–343.
26 S. Sivaraman, T. J. Sullivan, F. Johnson, P. Novichenok, G. Cui, C. Simmerling and P. J. Tonge, *J. Med. Chem.*, 2004, **47**, 509–518.
27 Q. Zhang and J. M. Takacs, *Org. Lett.*, 2008, **10**, 545–548.
28 L. Caviedes, J. Delgado and R. H. Gilman, *J. Clin. Microbiol.*, 2002, **40**, 1873–1874.
29 H. Bouazizi-Ben Messaoud, M. Guichard, P. Lawton, I. Delton and S. Azzouz-Maache, *Lipids*, 2017, **52**, 433–441.
30 H. Marrakchi, M.-A. Lanéelle and M. Daffé, *Chem. Biol.*, 2014, **21**, 67–85.
31 G. R. Labadie, A. de la Iglesia and H. R. Morbidoni, *Mol. Diversity*, 2011, **15**, 1017–1024.
32 L. A. Spagnuolo, S. Eltschkner, W. Yu, F. Daryaee, S. Davoodi, S. E. Knudson, E. K. Allen, J. Merino, A. Pschibul, B. Moree, N. Thivalapill, J. J. Truglio, J. Salafsky, R. A. Slayden, C. Kisker and P. J. Tonge, *J. Am. Chem. Soc.*, 2017, **139**, 3417–3429.
33 T. Sander, J. Freyss, M. von Korff and C. Rufener, *J. Chem. Inf. Model.*, 2015, **55**, 460–473.
34 J. H. McKerrow and C. A. Lipinski, *Int. J. Parasitol. Drugs Drug Resist.*, 2017, **7**, 248–249.
35 G. Abate, A. Aseffa, A. Selassie, S. Goshu, B. Fekade, D. WoldeMeskal and H. Miorner, *J. Clin. Microbiol.*, 2004, **42**, 871–873.
36 L. Bonnac, G. Y. Gao, L. Chen, K. Felczak, E. M. Bennett, H. Xu, T. Kim, N. Liu, H. Oh, P. J. Tonge and K. W. Pankiewicz, *Bioorg. Med. Chem. Lett.*, 2007, **17**, 4588–4591.
37 J. Mikus and D. Steverding, *Parasitol. Int.*, 2000, **48**, 265–269.
38 H. Babich and E. Borenfreund, *Appl. Environ. Microbiol.*, 1991, **57**, 2101–2103.

 This journal is © The Royal Society of Chemistry 2021